# Mechanistic simulations of kelp populations in a dynamic landscape of light, temperature, and winter storms

Szewczyk, Tim M; Moore, Pippa; Smale, Dan A.; Burrows, Michael; Adams, Thomas

*Published in:*
Ecological Modelling

*Publication date:*
2024

Ecological Modelling 488 (2024) 110590

Contents lists available at ScienceDirect

Ecological Modelling

journal homepage: www.elsevier.com/locate/ecolmodel

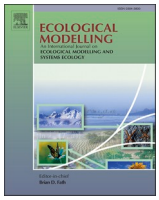

# Mechanistic simulations of kelp populations in a dynamic landscape of light, temperature, and winter storms

Tim M. Szewczyk [a,*], Pippa J. Moore [b], Dan A. Smale [c], Thomas Adams [d], Michael T. Burrows [a]

[a] The Scottish Association for Marine Science, SAMS, Dunbeg, Oban, Argyll PA37 1QA, UK
[b] The Dove Marine Laboratory, School of Natural and Environmental Sciences, Newcastle University, Newcastle-upon-Tyne NE1 7RU, UK
[c] The Laboratory, Marine Biological Association of the United Kingdom, Citadel Hill, Plymouth PL1 2PB, UK
[d] Scottish Sea Farms Ltd, Barcaldine, Argyll PA37 1SB, UK

ARTICLE INFO

*Keywords:*
Disturbance
Biomass
*Laminaria hyperborea*
Detrital production
Matrix model
Stochastic

ABSTRACT

Kelp forests are widely distributed across the coastal ocean, support high levels of biodiversity and primary productivity, and underpin a range of ecosystem services. *Laminaria hyperborea* is a forest-forming kelp species in the Northeast Atlantic that alters the local environment, providing biogenic structure for a diversity of associated organisms. Populations are strongly affected by light availability, temperature, and storm-related disturbance. We constructed a stage-based, two-season model of *L. hyperborea* populations along the coast of Great Britain and Ireland to predict biomass across a range of depths, drawing on extensive surveys and data from the literature. Population dynamics were driven by wave exposure, historic winter storm intensity, and simulated interannual variation in temperature and depth-attenuated light intensity, with density-dependent competition for light and space. High biomass was predicted in shallow depths across the domain on suitable substrate, with populations extending deeper in the north and west where light penetration was greater. Detritus production was heavily skewed across years, particularly at greater depths, with 10 % of years comprising more than 50 % of detritus on average below 10 m depth. Annual fluctuations in light and storm intensity produced opposing population oscillations with a ~6-year period persisting for up to a decade but diminishing sharply with depth. Interannual variation in temperature had minimal impact. Biomass was most sensitive to survival and settlement rates, with negligible sensitivity to individual growth rates. This model highlights the need for an improved understanding of canopy and subcanopy mortality, particularly regarding increasingly frequent heatwaves. Estimations of kelp forest contributions to carbon sequestration should consider the high variability among years or risk underestimating the potential value of kelp forests. Process-based simulations of populations with realistic spatio-temporal environmental variability are a valuable approach to forecasting biotic responses to an increasingly extreme climate.

## 1. Introduction

Kelp forests are among the most productive ecosystems on Earth, hosting diverse communities of microbes, flora, and fauna as well as forming key habitat for many socioeconomically important species (Bertocci et al., 2015; Christie et al., 2003; King et al., 2023; Steneck et al., 2002; Teagle et al., 2018). Found throughout temperate and subpolar coastlines, these large brown macroalgae provide important ecosystem services including nutrient cycling, carbon transfer, storm defence and fisheries habitat (Pessarrodona et al., 2018; Smale, 2020). In some regions, various species of kelp are harvested for commercial or personal use (Gouraguine et al., 2021; Steen et al., 2016; Westermeier et al., 2019). It is therefore important to understand the dynamics driving kelp forest structure and their resilience to disturbance events such as storms.

In the Northeast Atlantic, the kelp species *Laminaria hyperborea* forms extensive forests on subtidal (1–40 m below chart datum) rocky reefs on all but the most wave sheltered coastlines. The biomass of individual plants and the standing stock of the wider forest is highly variable over time and is influenced by natural growth cycles as well as environmental factors. Notably, winter storms driven by the North Atlantic Oscillation (Feser et al., 2021, 2015) cause increased frond erosion and dislodgement of whole plants (Filbee-Dexter and Scheibling, 2012; Kitching, 1937; Krumhansl and Scheibling, 2012;

* Corresponding author.
*E-mail address:* tim.szewczyk@sams.ac.uk (T.M. Szewczyk).

https://doi.org/10.1016/j.ecolmodel.2023.110590
Received 2 August 2023; Received in revised form 30 November 2023; Accepted 30 November 2023
Available online 6 December 2023

Pessarrodona et al., 2018; Smale et al., 2021; Walker, 1954). Wave disturbance can be extreme during intense storms and appears to drive local species distributions, with the more tolerant *L. hyperborea* occupying more exposed locations and the less tolerant *L. ochroleuca* and *Saccharina latissima* dominant in more sheltered areas (Smale and Vance, 2016). An emerging threat is the increase in marine heatwaves, which can lead to high mortality among cold-water kelp species such as *L. hyperborea*, particularly following repeated warming events (Filbee--Dexter et al., 2020; Hereward et al., 2020; Smale, 2020). Harvesting also introduces disturbance where techniques such as trawling are used (Burrows et al., 2018; Steen et al., 2016).

Light conditions within kelp forests are highly dynamic. For a given population, the light that reaches the canopy depends on the surface irradiance, depth, and light attenuation through the water. The light that reaches the substrate is further dependent on the canopy. Canopies are in constant movement in wave-exposed environments, increasing the light that reaches the subcanopy and substrate relative to comparable canopy densities in more wave-protected areas. Population dynamics are highly sensitive to light conditions due to canopy shading leading to intraspecific competition (Burgman and Gerard, 1990; Duarte and Ferreira, 1997; Nisbet and Bence, 1989; Pedersen et al., 2012). Seasonally, fronds grow and erode, a process that partially separates the shading impact of the canopy from the number of individuals in a patch. Notably, L. *hyperborea* sheds the growth from the previous year each spring in an event known as 'May cast'. Erosion occurs chronically throughout the year, though the rate may vary with environmental conditions (Aberg, 1992; Filbee-Dexter and Scheibling, 2012; Krumhansl and Scheibling, 2012; Pessarrodona et al., 2018). The resultant increase in light penetration through the thinned canopy drives an increase in successful recruitment and subcanopy growth (Duarte 1997).

Matrix model structures have been described for a range of detailed kelp life histories, including gametophyte and sporophyte stages, different sexes, and separation of discrete episodes of growth, reproduction, senescence, and regeneration (Ang and De Wreede, 1990). For kelp species with a dominant sporophyte stage, information on gametophyte dynamics is often sparse, and reproduction simplified to emphasize the sporophyte, with size- or age-based classification following available data (Aberg, 1992; Duarte and Ferreira, 1997; Nisbet and Bence, 1989; Pedersen et al., 2012) [but see (Burgman and Gerard, 1990; Pereira et al., 2017)]. Further, frond area is often the primary focus as fronds are centrally important to photosynthesis and carbon dynamics, and largely govern the proportion of light within the forest that reaches beyond the canopy, which in turn regulates establishment of new recruits and growth within the subcanopy (Broch et al., 2019; Broch and Slagstad, 2012; Krumhansl et al., 2014; Venolia et al., 2020).

Environmental stochasticity, widely recognised as an important factor in population dynamics (Shoemaker et al., 2020; Terry et al., 2022), is often included in population models as random noise about demographic rates (Morris et al., 2003). In part, this represents environmentally driven variation in these rates. In spatially explicit models where demographic parameters are linked to environmental conditions, however, such an implementation may overlook important realism. Directly implementing stochasticity via a dynamic environmental landscape incorporates spatiotemporal autocorrelation into the demographic rate variability, which propagates through to the population dynamics. Further, a given environmental variable may affect multiple demographic rates. A stochastic environmental landscape captures the resulting interannual correlation among those rates which would otherwise require careful treatment of suitably comprehensive datasets.

Here, we model populations of *L. hyperborea* on the coasts of Great Britain and Ireland to predict the dynamics of biomass across a range of environments and depths, aiming to improve our understanding of kelp population dynamics and to develop an empirical model to help inform management approaches. We draw on recent population surveys as well as data from the literature to construct a stage-based model driven by light availability, wave exposure and sea surface temperature, incorporating light-dependent growth and seasonal dynamics of canopy frond area. We explore the impact of annual variation in temperature and light regimes, as well as disturbance based on historical storm intensity in the North Atlantic.

## 2. Materials and methods

### 2.1. Study system

*Laminaria hyperborea* is a dominant kelp species found in the subtidal zone through much of the rocky coastline in the northeast Atlantic, including nearly all of the UK and Ireland (Kain, 1979, 1962; Pessarrodona et al., 2019; Smale et al., 2020). Its regional distribution is heavily shaped by temperature, while local variation is driven largely by light availability and wave exposure (Bekkby et al., 2019; Smale et al., 2020; Smith et al., 2022). *L. hyperborea* is composed of a holdfast that attaches to the substrate and a single rigid but flexible stipe that holds the single palmate frond up toward the water surface. Most growth occurs between January and June (Kain, 1976a, 1976b; Pessarrodona et al., 2019). Reproduction occurs primarily during the winter, involving the release of zoospores which attach to suitable rock surfaces, develop into gametophytes, and produce sperm and eggs that develop into sporophytes following successful fertilization (Kain, 1975).

To parameterize the model, we used a combination of *L. hyperborea* surveys and data previously published in the literature (Fig. A.1). Recent surveys were performed at a total of 22 locations, including sites along the southern, western, eastern, and northern coasts and islands of the UK (Catherall, unpublished; Smale et al., 2016; Smith et al., 2022). Surveys consisted of counting the number of canopy and subcanopy *L. hyperborea* individuals within 1 $m^2$ quadrats and collection of individuals for morphological measurements (e.g., total length/biomass, blade length/width/biomass, age) across a series of depths (2 – 15 m or where the kelp forest ended) at each site.

### 2.2. Model description

Kelp population dynamics were simulated using a size-based discrete time model, with recruits, subcanopy, and canopy classes, and density dependent growth and reproduction (Fig. 1, Table 1). All newly settled individuals were classified as recruits for their first year, after which surviving individuals grew into the subcanopy. Categorization into subcanopy or canopy was determined by stipe length. Light penetration through the canopy is a major determinant of *L. hyperborea* population dynamics (Bekkby et al., 2019; Desmond et al., 2017; Harrer et al., 2013; Smale et al., 2020; Smith et al., 2022; Wing et al., 1993). Because frond area – and consequently light limitation – varies through the year (Pessarrodona et al., 2019), we modelled frond dynamics interactively with population density and the stage distribution.

Annual population dynamics were partitioned into two transition matrices, representing seasonal timesteps with a population census at each transition. These matrices represent the primary growing season (January through June), during which nearly 90 % of growth occurs (Kain, 1976a; Pessarrodona et al., 2019), and the non-growing season (July through December) for *L. hyperborea* in the region. Growing season dynamics include growth in stipe length and frond area, as well as mortality. Non-growing season dynamics include loss of frond area, mortality, and reproduction. Simulations were thus performed with two time steps per year.

Canopy height varies dramatically throughout the geographic range of *L. hyperborea* (Pessarrodona et al., 2018), with shorter plants at warmer temperatures. Canopy height was predicted in each cell using a linear regression with average environmental conditions instead of emerging from simulated growth (Table A.1), with the height of the subcanopy calculated as a proportion of the canopy height. We assume

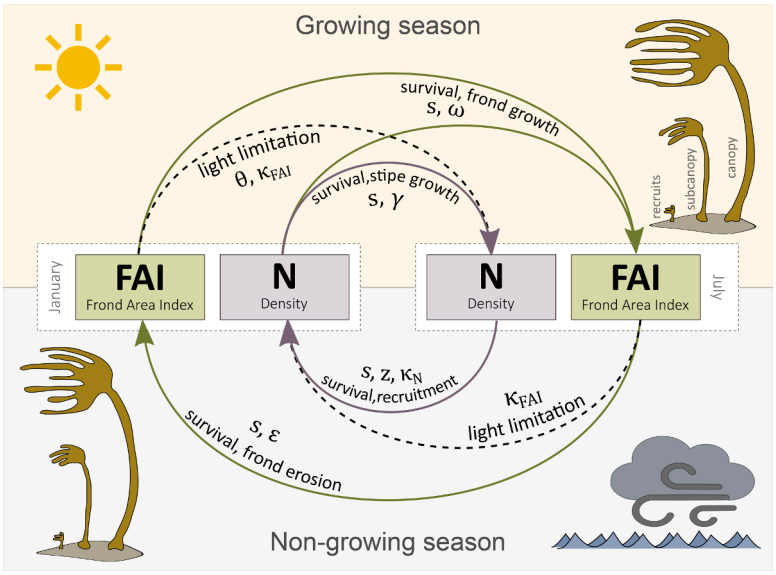


**Fig. 1.** Model structure. Kelp density and frond dynamics were modelled using three stages (recruits, sub-canopy, canopy), with each year divided into growing (Jan-Jul) and non-growing (Jul-Jan) seasons. Growth between stages was regulated via light limitation by the canopy, while recruitment was limited both by light and abundance. During the non-growing season, survival and frond erosion were driven by historic storm severity.

**Table 1**
List of population dynamics equations. See text for detailed descriptions.

| Equation | Description |
|---|---|
| $p_{ji} = g_{ji}s_i$ | Transition probability from $i$ to $j$ |
| $g_{ji} = \frac{\gamma_i(1-\kappa_{FAI,t}^{\theta})}{\delta_{ji}}$ | Probability of growth from $i$ to $j$ |
| $p_{ii} = s_i - p_{ji}$ | Probability of remaining in $i$ |
| $FAI_{t+1} = N_{cnpy,t}p_{cnpy,cnpy}\omega(1-\kappa_{FAI,t}) + N_{sbcnpy,t}p_{cnpy,sbcnpy}A_{cnpy}$ | Canopy frond area index during the growing season |
| $FAI_{t+1} = FAI_t(p_{cnpy,cnpy} - \varepsilon)$ | Canopy frond area index during the non-growing season |
| $N_{rcr,t+1} = z(1-\max(\kappa_{FAI,t},\kappa_{N,t}))$ | Realized settlement rate |

that individual growth rates are identical among populations, and consequently individuals are expected to reach the canopy at a younger age in warmer waters where canopy height is shorter (Kain, 1963).

### 2.2.1. Growing season

Population processes during the growing season consist of stipe growth, frond growth, and survival. The transition between recruit, subcanopy, and canopy stages is governed by stipe growth (Duarte and Ferreira, 1997). The transition probability from stage $i$ to stage $j$ during the growing season is calculated as:

$$p_{ji} = g_{ji}s_i$$

$$g_{ji} = \frac{\gamma_i\left(1-\kappa_{FAI,t}^{\theta}\right)}{\delta_{ji}}$$

where $s_i$ is the probability of survival, $g_{ji}$ is the probability of growth from stage $i$ to stage $j$, $\gamma_i$ is the maximum growth rate, $\kappa_{FAI,t}$ is $\frac{FAI_t}{FAI_K}$ representing the canopy Frond Area Index at the start of the growing season as a proportion of the predicted maximum FAI given environmental conditions, $\delta_{ji}$ is the stipe length increase necessary to reach class $j$, and $\theta$ is a shape parameter for the effect of canopy density on the growth rate, following the form of theta-logistic population growth (Gilpin and Ayala, 1973). We assume asymmetric competition for light, such that the frond area of the canopy limits the growth of the subcanopy and recruit stages. The expected maximum FAI in each cell, $FAI_K$, is predicted by light availability and wave exposure (Table A.1).

The probability of remaining in the same stage is:

$$p_{ii} = s_i - p_{ji}$$

where $p_{ji} = 0$ for canopy plants. We assume the survival rate is constant within a stage and unaffected by density. Subcanopy individuals may thus persist under dense canopy for years, consistent with field observations (*unpublished*).

When individuals reach the canopy, initial frond area is calculated allometrically based on the midpoint of the stipe length (Kain, 1977). Subsequent dynamics are modelled based on frond growth and erosion. The frond area of the canopy at the end of the growing season is calculated as the sum of the net growth in frond area of surviving individuals and the frond area of the individuals that grew from the subcanopy to the canopy:

$$FAI_{t+1} = N_{cnpy,t}p_{cnpy,cnpy}\omega\left(1-\kappa_{FAI,t}\right) + N_{sbcnpy,t}p_{cnpy,sbcnpy}A_{cnpy}$$

where $FAI_{t+1}$ is the canopy Frond Area Index at the end of the growing season, $N$ is abundance at the start of the growing season, $\omega$ is the maximum frond area growth rate, and $A$ is the allometrically calculated frond area per individual. Because 'May cast' occurs during the growing season, the frond area remaining at the end of the growing season is composed only of new growth. Additionally, chronic erosion of the lamina occurs throughout the year (Pessarrodona et al., 2018), which is accounted for in the maximum growth rate $\omega$.

### 2.2.2. Non-growing season

Dynamics during the non-growing season are characterized by mortality, erosion of the frond, and reproduction. While stipe lengths remain constant, frond area is lost, reducing the canopy cover more than would be expected based solely on survival. We assume that erosion of the frond occurs proportionally to the frond area:

$$FAI_{t+1} = FAI_t\left(p_{cnpy,cnpy} - \varepsilon\right)$$

where $\varepsilon$ is the proportional chronic erosion rate which is constrained to $[0, p_{ii}]$. As during the growing season, frond dynamics are only modelled for the canopy. Since no stage transitions occur, $p_{ii} = s_i$ for all stages. In contrast to the invariant survival rates during the growing season, survival and erosion rates during the non-growing season are determined by winter storm intensity which varies among years (Fig. A.4).

Recruitment is assumed to occur with open settlement, such that zoospores are well-mixed on relevant spatial scales through the ocean currents (Roughgarden et al., 1985). Consequently, the number of potential recruits is constant and unrelated to local densities. However, the realized settlement rate is dependent on the availability of light and space:

$$N_{rcr,t+1} = z\left(1 - \max\left(\kappa_{FAI,t}, \kappa_{N,t}\right)\right)$$

where $z$ is the potential number of recruits and $\kappa_{N,t}$ is $\frac{N_{cnpy,t}}{N_K}$ representing canopy abundance at the start of the non-growing season as a proportion of the predicted maximum canopy abundance given environmental conditions. The expected maximum abundance in each cell, $N_K$, is predicted by light availability, sea surface temperature, and wave exposure (Table A.1). Recruitment in any given year is thus constrained by the most limiting factor.

### 2.3. Landscape

We simulated populations on a 0.1° grid around the coast of Great Britain, including all areas with depth less than 40 m within 5 km of the coast (GEBCO, 2021). For each simulated depth in each cell, dynamics of *L. hyperborea* were driven by wave exposure, photosynthetically available radiation (PAR), sea surface temperature, and winter storm intensity (Fig. 2; Fig. A.6).

Wave exposure was included as log-10 transformed wave fetch calculated on a 200 m grid (Burrows, 2012; Burrows et al., 2008) restricted to locations with a depth less than 40 m, and then averaged within each grid cell. Average wave fetch was used as a continuous variable in linear regressions. For survival and recruitment rates, the average wave fetch within each grid cell was categorized as low or high using thresholds calculated from the site locations provided in Pedersen et al. (2012) to align with the categorized source data (Fig. A.7). Slope was additionally calculated based on bathymetry but was highly correlated with fetch once aggregated to the grid ($r = 0.96$) and therefore not included.

Temperature and depth-specific light availability were estimated using MODIS-Aqua products (annual average for Jan-June 2003–2021; resolution 4 km (NASA, 2018)). Specifically, we used the daytime sea surface temperature at 11 μm, the surface PAR, and the diffuse coefficient for downwelling irradiance at 490 nm. Within each grid cell, we first calculated the Jan-June mean by year for each variable, then the mean and standard deviation across years. The PAR at each depth $d$ in each cell was then calculated as $PAR_d = PAR_0 e^{-K_D d}$, with surface radiation $PAR_0$ and diffuse attenuation coefficient $K_D$.

The intensity and frequency of winter storms varies among years, driven in large part by the North Atlantic Oscillation (Feser et al., 2021, 2015). Increased storms are expected to impact kelp populations both through increased frond erosion and through increased mortality via dislodgement of entire plants. To simulate interannual variation in storms, we used a standardized storm index based on the 95th percentiles of geostrophic wind speed in the North Atlantic for a 76-year timeseries from 1943 to 2018 (Feser et al., 2021) (Fig. A.3). The non-growing season survival and erosion rates were calculated in each year by applying the storm index quantile to the respective distributions, such that a higher storm index translated to commensurately higher frond loss and mortality (Fig. A.4). Survival rates during the growing season were unaffected.

Environmental stochasticity was incorporated through the generation of a dynamic environment (Fig. 2b) (Denny et al., 2009; Morris et al., 2003). In each year, sea surface temperature, surface PAR, and attenuation were generated for each cell using the mean across years and the covariance matrix to account for correlation among cells, with attenuation coefficients treated on a log scale. Values were simulated from a multivariate normal distribution for each variable across years, preserving the spatial correlation observed in each variable. We assumed that environmental variables fluctuated across years independently of one another. We simulated 200 landscape timeseries, each corresponding to the 76-year length of the storm severity timeseries.

### 2.4. Parameterization

We estimated parameter values (Table A.2, Fig. A.5) and fit regressions (Table A.1, Fig. A.2) using *L. hyperborea* survey data collected across five regions of the UK as well as data from the literature (Fig. A.1), with a preference for UK localities where possible. In each case, we estimated distributions representing plausible ranges of values, or used Bayesian methods to incorporate uncertainty in the relationships via the posterior distributions (Fig. 2a). For best estimates used in the simulations, we used the means of the corresponding parameter distributions and the mean of the posterior distributions from the Bayesian models.

Maximum stipe growth rates for each stage, $\gamma_i$, were calculated using data from a clearing experiment which reported average daily growth

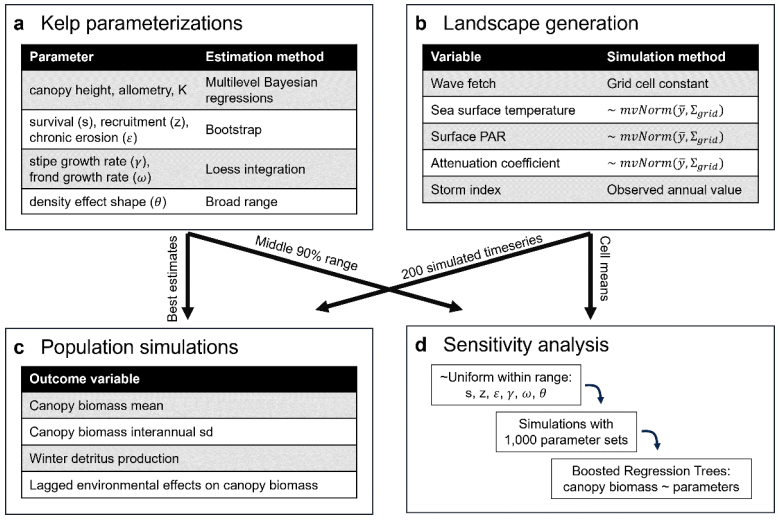


**Fig. 2.** Methodology overview. (a) Kelp population parameters were estimated from several data sources using statistical methods corresponding with each data type (Table A.1, A.2). (b) Annually dynamic landscapes were simulated using cell means and correlations among cells based on satellite derived products. (c) Population simulations used best estimates of each population parameter and 200 independent simulated landscape timeseries. (d) The sensitivity analysis used the mean landscape with varying population parameter values to identify the relative influence of each parameter on the canopy biomass in each cell and depth.

rates by date (Kain, 1976a). Data were reported by age and were therefore categorized to approximate stage with recruits as age 0, subcanopy as ages 1–3, and canopy as ages 3–4. Seasonal totals were estimated by fitting loess lines to each stage and integrating under the curve from January through June. The uncertainty was estimated using the standard error of the loess regression. We explored a range for the density effect shape parameter, $\theta$, that centered on a linear effect of density on growth rates but spanned from concave to convex.

Maximum frond growth rate for the canopy, $\omega$, was calculated similarly, by integrating over the growing season under a loess regression line fitted to data from the same clearing experiments of daily frond area growth rates per individual (Kain, 1976a). The same age ranges as for stipe growth were used to categorize ages into stages.

The survival rate for each stage, $s_i$, varied by exposure category following values from populations in Norway (Pedersen et al., 2012). Sites were categorized by wave fetch, with original medium and high exposure sites combined to better correspond with the distribution of exposure in the UK (Fig. A.6, Fig. A.7). We used bootstrapping to generate densities and mortalities for each stage and exposure, then fit beta distributions to estimate survival rates.

Settlement rates, $z$, for each exposure category were estimated similarly to survival rates using the same data source and aggregation (Pedersen et al., 2012). We then fit normal distributions truncated at 0 for each exposure category.

The chronic erosion rate, $\epsilon$, was estimated based on monthly loss and accumulation rates for *L. hyperborea* in southwest England (Pessarrodona et al., 2019). We used bootstrapping to generate distributions of loss as a proportion of growing season accumulation, excluding months with elevated loss indicating May cast. We then fit a beta distribution to estimate the erosion during the non-growing season as a proportion of the growing season accumulation.

Bayesian regressions were used to link height-based stages to biomass and frond dynamics, incorporating environmental relationships with previous support in the literature (Table A.1). Stipe weight was calculated from stipe length and wave fetch, allowing relatively stouter stipes in more exposed environments with increased wave action (Bekkby et al., 2014; Duggins et al., 2003; Koehl et al., 2008; Sjøtun and Fredriksen, 1995; Wernberg and Vanderklift, 2010). The relationship between frond weight and area was contingent on PAR, as frond thickness has been found to decrease with depth, presumably the result of decreased illumination (Kain, 1977, 1963). All relationships were modelled as linear on a log-log scale.

### 2.5. Analysis

We analysed several aspects of the population simulations with dynamic landscapes (Fig. 2c). For each cell and depth, the mean and standard deviation of canopy biomass across years was calculated to assess general spatial patterns.

To assess the impact of environmental drivers on population dynamics through time, we performed simple linear regressions of canopy biomass with each environmental variable, lagged from 1 to 15 years. All variables were standardised within each cell and depth to allow for direct comparison of effect magnitudes. For each cell and depth, we calculated the amplitude of the effect of each variable as the difference in the maximum and minimum slopes across lags.

Annual winter detritus production was calculated for each cell and depth as the difference in canopy mass between the start and end of each non-growing season. Detritus thus includes both frond erosion and dislodgement of whole plants. The percent loss was calculated using the canopy biomass at the start of the non-growing season. Within each cell and depth, years were classified into deciles based on mass of detritus. The proportional distribution of total detritus among deciles was then calculated.

### 2.6. Sensitivity analysis

To assess the effect of each parameter on the population dynamics, we performed a global sensitivity analysis (Fig. 2d) (Aiello-Lammens and Akçakaya, 2017; Prowse et al., 2016; Szewczyk et al., 2019). For each parameter (survival rates, settlement, erosion rate, frond growth rate, and stipe growth rate), we identified data-driven 90 % plausible ranges (Table A.2, Fig. A.5). In a global sensitivity analysis, all parameters are varied simultaneously and independently such that the effect of each is marginalized across all others to capture potential interactions. For computational purposes, the sensitivity analysis was performed using a static landscape of mean values. We drew 1000 sets of parameters, simulated populations, and calculated mean and standard deviation across years for canopy biomass.

To assess the relative importance of each parameter, we used boosted regression trees (BRTs), including all varied parameters as predictors and with separate analyses for each population metric in each cell (Elith et al., 2008; Prowse et al., 2016; Szewczyk et al., 2019). BRTs are a machine learning approach that creates an ensemble model of regression trees optimized for predictive performance. The relative influence of each parameter can be calculated based on the weights of the regression trees included in the ensemble model (Elith et al., 2008). We assessed tree complexities of 1, 3, and 5, and fit each BRT with bootstrapped subsets of the simulations using cross-validation deviance and relative influence stability across subsets to ensure adequate exploration of the parameter space (Prowse et al., 2016; Szewczyk et al., 2019).

### 2.7. Modelling details

We simulated populations at 2, 5, 10, 15, and 20 m depth in each cell of the landscape for 76 years. Data processing, simulations, and analysis were performed in R 4.1.2 using the R packages *sf* (1.0.7), *raster* (3.5.15), *stars* (0.5.5), *lubridate* (1.8.0), *fitdistrplus* (1.1.8), *mvtnorm* (1.1.3), *parallel* (4.1.2), *dismo* (1.3.5), *gbm* (2.1.8), and *brms* (2.16.3), as well as those included in *tidyverse* (1.3.1). All code is available at https://doi.org/10.5281/zenodo.8205599.

## 3. Results

In shallow water, *Laminaria hyperborea* canopy biomass (Fig. 3a) was predicted to be high across the domain on suitable substrate (2 m mean: 12.0 kg/m$^2$, middle 90 %: 5.44–17.8 kg/m$^2$). Mean biomass was higher along the northern and western coasts and islands, and somewhat lower in the south and east. Biomass declined with depth, but less dramatically on the west coast of Scotland, Orkney, and Shetland. Interannual variability in canopy biomass generally followed an inverse relationship with mean biomass, such that populations with lower mean biomass showed higher proportional variability among years (Fig. 3b, Fig. B.1). Interannual variability was also higher among more wave exposed populations. Turnover of canopy biomass was high during the non-growing season, with an average loss of 35.0–39.4 % across depths due to mortality (dislodgement) and frond erosion, though with high variability among years and cells (2 m mean: 4.75 kg/m$^2$, 39.4 %; middle 90 %: 0.674–10.8 kg/m$^2$, 15.4–67.4 %; 5 m mean: 2.44 kg/m$^2$, 37.4 %; middle 90 %: 0.0323–7.2 kg/m$^2$, 15.2–63.0 %). Skewness among years increased with depth, such that the most extreme 10 % of years accounted for an average of 23.7 % of total loss at 2 m, but 51.5 % at 10 m (Fig. 4; Fisher's moment coefficient of skewness, mean among cells at 2m: 1.18, at 10m: 3.95).

In this model, populations developed within a dynamic landscape with annual variability in winter storm intensity, depth-attenuated PAR, and sea surface temperatures. The impact of variation in each environmental variable depended on the depth of the kelp population. Fluctuations in the environmental conditions initiated population oscillations that persisted for up to a decade (Fig. 5). Annual variation in SST had minimal effect, while PAR and storm intensity showed opposing effects

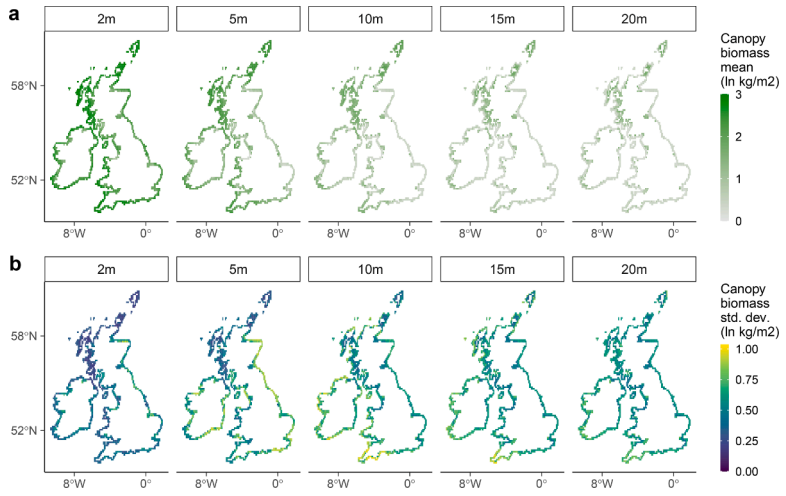


**Fig. 3.** Geographic patterns in predicted biomass. (a) Mean canopy biomass in July is high across the domain at shallow depths, decreasing with depth particularly in the east and south. (b) Interannual standard deviation in July biomass generally increases with depth, with typically greater variability in southwestern England.

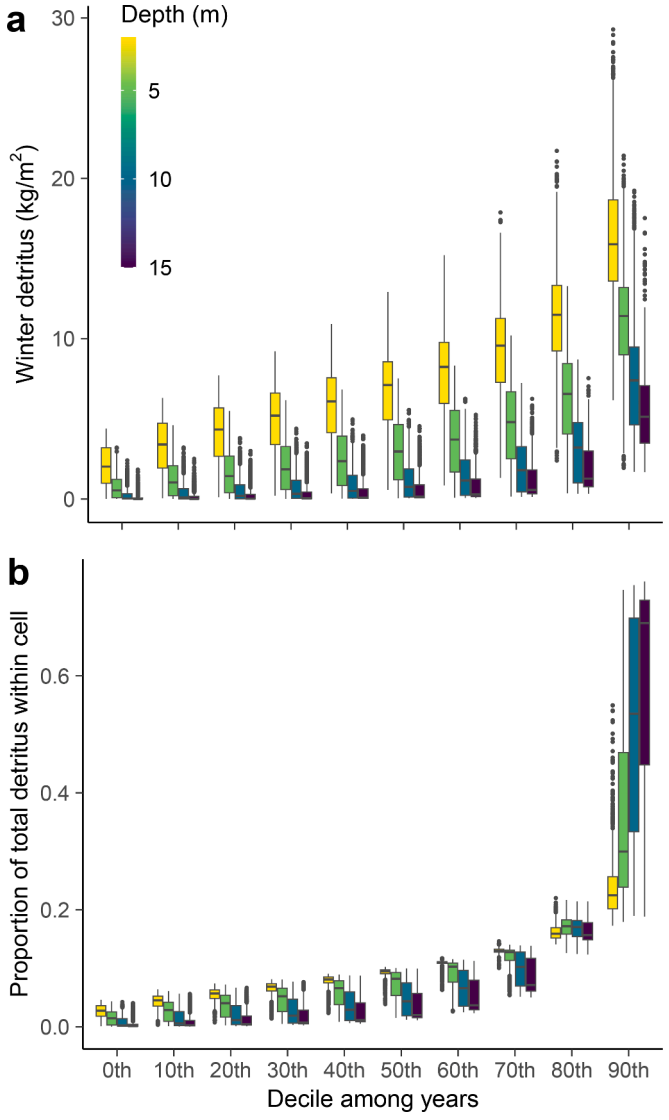


**Fig. 4.** Interannual variation in detritus production. (a) Shallower populations produced more detritus, reflecting the higher canopy biomass. (b) Detritus production became increasingly skewed among years with increased depth.

of comparable magnitude, each driving oscillations with a period of approximately 6–8 years. That is, high PAR caused initial increases in canopy biomass while high storm intensity caused initial decreases; in years 4–6, canopy biomass then decreased or increased, respectively, as the oscillations dampened. The sensitivity to both variables declined sharply with increased depth.

The effects of environmental variability also depended on geographic location (Fig. B.4). The largest amplitude of the oscillatory effect (i.e., difference between the maximum and minimum across lags) occurred in response to storm intensity at shallow depth in the north and west of Scotland. In this region, storm effect amplitude was higher for low exposure cells. Response to PAR was less geographically variable, though tended to be somewhat stronger in the north and west as well, particularly for deeper populations. Subcanopy abundance showed similar relative patterns, with somewhat greater PAR effect amplitudes (Fig. B.3b, Fig. B.4b). In contrast, recruit abundance was extremely responsive to fluctuations in PAR along the east coast of the UK and minimally impacted elsewhere (Fig. B.3a, Fig. B.4a).

Across all populations, mean biomass was most sensitive to settlement rate ($z$: 22.5 ± 6.9 %; mean relative influence ± sd) and survival rates ($s$: recruits: 14.5 ± 4.0 %; subcanopy: 21.4 ± 13.2 %; canopy: 18.6 ± 12.3 %), with moderate sensitivity to the chronic erosion rate ($\varepsilon$: 9.2 ± 8 %) and the density effect shape parameter ($\theta$: 7.6 ± 3.7 %) (Fig. 6). Biomass showed little sensitivity to stipe or frond growth rates ($\gamma$, $\omega$: < 2 %). As depth increased, the relative influence of canopy survival increased, and that of subcanopy survival decreased. Interannual standard deviation in biomass was driven by the same parameters, though with less sensitivity to depth.

Sensitivity to each parameter also varied across geography, dependent on the environmental conditions at each location (Fig. 7). Shallow populations in the east and south tended to show greater sensitivity to the canopy survival rate compared to northern or western populations which were more sensitive to subcanopy survival. Further, wave-sheltered populations were more sensitive to canopy survival, particularly at greater depths, and to subcanopy survival across all depths (Fig. B.5). More wave-exposed populations showed higher relative influence of the settlement rate and density effect shape parameter compared to less exposed populations. In high exposure populations, sensitivity to the erosion rate declined with depth, while it increased on average with depth in low exposure populations. Similarly, the relative importance of recruit survival increased with depth at high exposure and decreased somewhat with depth at low exposure.

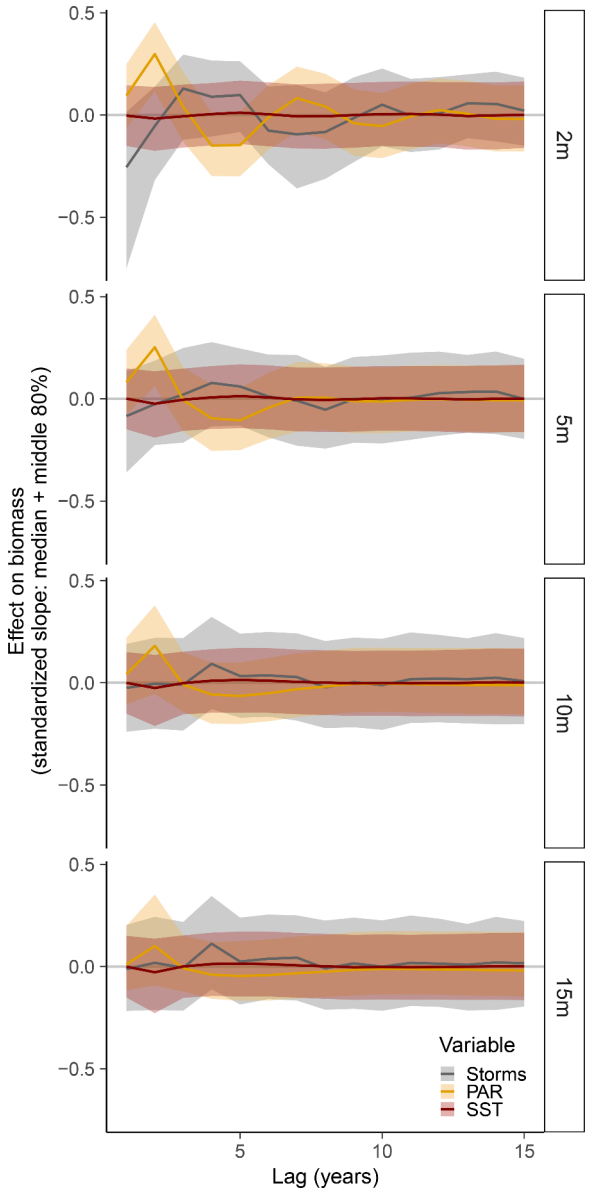


**Fig. 5.** Lagged effect of environmental variables on median biomass. The oscillations caused by interannual variation in environmental drivers diminish with depth.

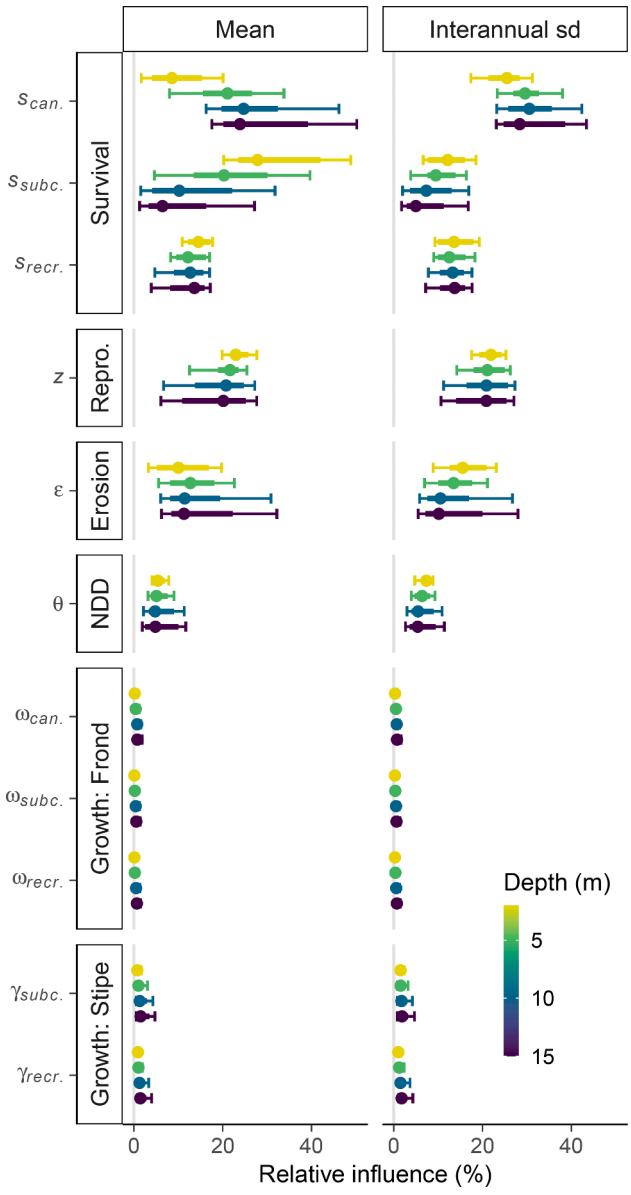


**Fig. 6.** Sensitivity analysis landscape summary. Relative influence of each parameter on biomass mean and interannual standard deviation across populations (point: median; thick bar: middle 50 %; whiskers: middle 90 %).

## 4. Discussion

*Laminaria hyperborea* canopy biomass was predicted to be high in shallow waters on suitable substrate throughout the UK, decreasing with depth more rapidly in the south and east than in the north and west. This geographic difference was largely driven by the combination of relatively high light availability in the north at greater depths (Fig. A.6c) and the taller, heavier individuals that compose the canopy at colder temperatures (Fig. A.2e). These broad patterns are consistent with empirical patterns in the UK (Smith et al., 2022) and previous findings regarding the environmental drivers of *L. hyperborea* (Bekkby et al., 2019).

Photosynthetically active radiation (PAR) and storm intensity were major drivers of temporal variability in canopy biomass, each producing oscillations with a period of 6–8 years. While the effects of storms and PAR were comparable on average across the landscape, the most environmentally responsive populations exhibited greater sensitivity to storm intensity. These high biomass populations, concentrated in the north and west of Scotland, were also particularly sensitive to survival rates, which are directly linked to storm intensity and only indirectly to PAR.

This response mirrors the high canopy abundances observed in *L. hyperborea* forests approximately 3 years after clearances in the UK (Kain, 1976a) and Norway (Christie et al., 1998; Sjøtun et al., 2006). Within kelp forests, high canopy survival rates and correspondingly long lifespans maintained canopy densities with only limited recruitment. Following canopy clearing, however, the resultant increase in light led to increased recruitment and subcanopy survival (Sjøtun et al., 2006). The model presented here replicates this resilience and suggests a high potential for ephemeral populations to persist in areas where conditions are, on average, marginal via temporal variability in environmental conditions creating adequate conditions periodically allowing successful establishment (Christie et al., 2019; Dayton, 1985). Note, however, that communities associated with *L. hyperborea* forests were not modelled, and would almost certainly re-establish considerably more slowly as has been seen in experimental trawling of *L. hyperborea* where epiphytes had

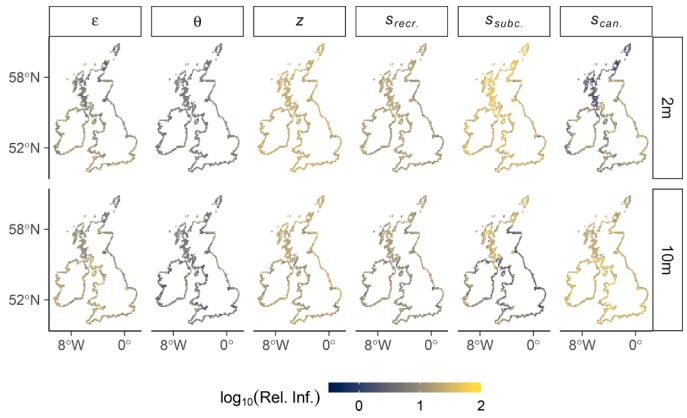


**Fig. 7.** Geographic variation in parameter relative influence. Maps of relative influence for mean July biomass at 2 m and 10 m depth. Only parameters with relative influence > 10 % in at least one population are shown (frond erosion rate ε, density dependence shape $\theta$, settlement rate $z$, and survival rates $s$).

not fully recovered after 6 years (Christie et al., 1998).

The average simulated annual detritus production aligned well with observations in the UK (Smale et al., 2021). While modelled carrying capacities incorporated observations from these locations, survival and chronic erosion rates were estimated from independent sources. As highly productive ecosystems, kelp forests may contribute to the removal of carbon via the generation of detritus that is then transported to sink locations such as the deep ocean (Krumhansl and Scheibling, 2012; Pedersen et al., 2021; Smale et al., 2021). The ultimate fate of the detritus thus depends heavily on the marine hydrodynamic landscape which varies intra- and interannually (van Sebille et al., 2018). Dynamic simulations of kelp populations, situated within ocean hydrodynamic models, offer an opportunity to align the high dislodgement rates associated with winter storms in the UK with expected transport of the debris (Aleynik et al., 2017; Broch et al., 2022). Detritus production in our simulations was highly skewed across years, particularly in deeper populations. Calculations of the potential contribution of kelp forests to carbon storage would benefit from accounting for this interannual variability, as values calculated from a short timeseries are unlikely to capture the high-production years that account for a large proportion of the long-term detritus production of *L. hyperborea* forests.

Recruitment was assumed to be open, with the number of potential recruits unrelated to the local population size. The constant supply of potential zoospores aided in rapid recovery of the canopy (~3 years) following a disturbance. While recovery of the physical forest structure within 3–6 years is consistent with observed recoveries following trawling (Christie et al., 1998), the generalizability of this timescale depends on the spatial scale of the disturbance, as well as the combination of currents, bathymetry, and the distribution of kelp populations in the surrounding area. In fact, there is quite a lot of variability in the literature regarding zoospore dispersal distances. *L. hyperborea* zoospores were found to be abundant in the water column as far as 200 m from the nearest populations (Fredriksen et al., 1995), and have been found up to 5 km from the nearest known adult plants (Norton, 1992). Dispersal kernels are thus quite fat-tailed, leading to more rapid recovery and colonization than may otherwise be expected by average dispersal distances. For instance, despite mean dispersal distances of 25 m (Capdevila et al., 2018), *Macrocystis pyrifera* spores have been found to travel several kilometers, allowing ready recolonisation of patches as far as 3.5 km from the nearest known source (Reed et al., 2006, 2004). For *L. hyperborea* in wave exposed locations of the UK and Ireland, winter storms in particular may greatly increase transport distances (Norton, 1992; Reed et al., 1988). The assumption of open recruitment in *L. hyperborea* is therefore reasonable at moderate spatial resolutions and at seasonal timescales, during which sporadic long-distance dispersal events are likely to occur.

Mean canopy biomass showed highest sensitivity to survival and reproduction, with intermediate sensitivity to the chronic frond erosion rate and shape of the density dependence parameter, and minimal impact of stipe or frond growth rates. Further, sensitivity to survival rates varied by depth, such that shallow populations were more sensitive to subcanopy survival rates while deep populations were more sensitive to canopy survival rates. This depth-dependence reflects the impact of interannual variation in light availability. In deep water, conditions are favourable for recruitment only occasionally. These infrequent cohorts that become established allow the population to persist for several years depending on the canopy survival rate. In contrast, shallow populations see consistent recruitment across years. The subcanopy survival rate thus determines the density of individuals present to grow into a clearing in the canopy. The sensitivity analysis indicates that future work on *L. hyperborea* would be most improved by more extensive data relating to survival and recruitment rates rather than individual growth rates.

Though temperature drove an increase in canopy biomass with latitude via its effect on canopy height, interannual variability in temperature had little impact on canopy biomass, reflecting its modest slopes in the vital rate regressions. Nevertheless, heatwaves are known to cause mortality in cold water kelp species such as *L. hyperborea* (Filbee-Dexter et al., 2020; Hereward et al., 2020; Smale, 2020). There are three likely reasons why these simulations failed to capture such events. First, data limitations prevented including temperature as a predictor of survival. Second, heatwaves may be short-term events that are not captured by seasonal averages. Third, given that these populations fall within the range center of *L. hyperborea,* which extends southwards to the Iberian Peninsula, absolute temperatures experienced may not be stressful enough to manifest as changes in population structure. The minimal effect of temperature thus reflects data-based compromises within the model, highlighting a key area for future research particularly given the sensitivity of canopy biomass to canopy and subcanopy survival rates. Process-based simulations offer a promising approach for incorporating cumulative effects of heat stress, intra- and inter-annual environmental variability, and the potential for local adaptation, given corresponding empirical work. For species or systems where appropriate data are available, this modelling framework is amenable to including chemical aspects of the environment like nutrients which have established physiological links to kelp growth (Bolton and Lüning, 1982).

These simulations imposed environmental stochasticity via stochastic variability in the environment rather than in the parameters. Variability in environmental conditions drove variability in biological processes, which in turn produced biomass dynamics. This approach, where a process-based model is combined with a stochastic environment, captures correlation in vital rates that would otherwise require stricter assumptions for simulating covariance or potentially burdensome experiments to parameterize (Hilde et al., 2020; Shoemaker et al., 2020). For example, recruitment success and subcanopy growth rates each depend on light availability (Desmond et al., 2017; Kain, 1969), and would thus be expected to covary based on interannual variation in PAR. Here, each parameter was predicted based on PAR and other relevant variables, creating an implicitly correlated deterministic component with residual error simulated via Bayesian posterior distributions. Further, realistic spatial correlation is much simpler to capture in environmental conditions using satellite-derived products as opposed to geographically extensive field experiments. This approach could be especially valuable when simulating future population trajectories to incorporate more realistic impacts of interannual variability in the context of shifting averages.

## 5. Conclusions

Here, we leverage a diversity of data sources to simulate the dynamics of a key kelp species in the Northeast Atlantic in a realistic

landscape of light, temperature, and winter storms. Combining a spatiotemporally dynamic environment with process-based population dynamics illustrated the interplay between demographic rates, life stages, and persistent environmental impacts. Fluctuations in storm intensity and light availability each induced population oscillations with a period of ~6 years, suggesting the potential for resilience following disturbance, provided the depleted population is within the range of dispersal of neighboring populations. Further empirical work on survival and recruitment is likely to be most impactful, particularly with regard to increasingly frequent and intense marine heatwaves. These simulations further illustrate the importance of considering spatiotemporal variation in growth and detritus production in the context of carbon budget calculations. As the climate continues to change, process-based models that include realistic environmental variation will become increasingly important tools for understanding and predicting biological change.

## CRediT authorship contribution statement

**Tim M. Szewczyk:** Formal analysis, Investigation, Methodology, Software, Validation, Visualization, Writing – original draft, Writing – review & editing. **Pippa J. Moore:** Conceptualization, Data curation, Investigation, Methodology, Project administration, Resources, Writing – original draft, Writing – review & editing. **Dan A. Smale:** Conceptualization, Data curation, Funding acquisition, Investigation, Methodology, Project administration, Resources, Writing – original draft, Writing – review & editing. **Thomas Adams:** Conceptualization, Funding acquisition, Investigation, Methodology, Resources, Software, Writing – original draft, Writing – review & editing. **Michael T. Burrows:** Conceptualization, Formal analysis, Funding acquisition, Investigation, Methodology, Project administration, Resources, Software, Writing – original draft, Writing – review & editing.

## Declaration of Competing Interest

The authors declare that they have no known competing financial interests or personal relationships that could have appeared to influence the work reported in this paper.

## Data availability

All data are available in the public repository at: https://doi.org/10.5281/zenodo.8205599.

## Acknowledgements

This work was supported by NERC [grant numbers NE/S011692/1 and NE/S011692/2]. DAS was supported by a UKRI Future Leaders Fellowship (MR/S032827/1). We thank all participants of “Team Kelp (UK)” field expeditions (2014–2021), and Sula Divers, In Deep, NFSD and Tritonia dive teams for technical field support.

## Appendices

Appendix A. Supplemental methods
Appendix B. Supplemental results

## Supplementary materials

Supplementary material associated with this article can be found, in the online version, at doi:10.1016/j.ecolmodel.2023.110590.

## References

Aberg, P., 1992. A demographic study of two populations of the seaweed Ascophyllum nodosum. Ecology 73, 1473–1487. https://doi.org/10.2307/1940691.
Aiello-Lammens, M.E., Akçakaya, H.R., 2017. Using global sensitivity analysis of demographic models for ecological impact assessment. Conserv. Biol. 31, 116–125. https://doi.org/10.1111/cobi.12726.
Aleynik, D., Adams, T., Davidson, K., Dale, A., Porter, M., Black, K., Burrows, M., 2017. Biophysical Modelling of Marine Organisms: Fundamentals and Applications to Management of Coastal Waters. Environmental Management of Marine Ecosystems. CRC Press, ISBN 978-1-315-15393-3.
Ang, P., De Wreede, R., 1990. Matrix models for algal life history stages. Mar. Ecol. Prog. Ser. 59, 171–181. https://doi.org/10.3354/meps059171.
Bekkby, T., Rinde, E., Gundersen, H., Norderhaug, K., Gitmark, J., Christie, H., 2014. Length, strength and water flow: relative importance of wave and current exposure on morphology in kelp Laminaria hyperborea. Mar. Ecol. Prog. Ser. 506, 61–70. https://doi.org/10.3354/meps10778.
Bekkby, T., Smit, C., Gundersen, H., Rinde, E., Steen, H., Tveiten, L., Gitmark, J.K., Fredriksen, S., Albretsen, J., Christie, H., 2019. The abundance of kelp is modified by the combined impact of depth, waves and currents. Front. Mar. Sci. 6, 475. https://doi.org/10.3389/fmars.2019.00475.
Bertocci, I., Araújo, R., Oliveira, P., Sousa-Pinto, I., 2015. REVIEW: potential effects of kelp species on local fisheries. J. Appl. Ecol. 52, 1216–1226. https://doi.org/10.1111/1365-2664.12483.
Bolton, J.J., Lüning, K., 1982. Optimal growth and maximal survival temperatures of Atlantic Laminaria species (Phaeophyta) in culture. Mar. Biol. 66, 89–94. https://doi.org/10.1007/BF00397259.
Broch, O.J., Alver, M.O., Bekkby, T., Gundersen, H., Forbord, S., Handå, A., Skjermo, J., Hancke, K., 2019. The kelp cultivation potential in coastal and offshore regions of Norway. Front. Mar. Sci. 5, 529. https://doi.org/10.3389/fmars.2018.00529.
Broch, O.J., Hancke, K., Ellingsen, I.H., 2022. Dispersal and deposition of detritus from kelp cultivation. Front. Mar. Sci. 9, 840531 https://doi.org/10.3389/fmars.2022.840531.
Broch, O.J., Slagstad, D., 2012. Modelling seasonal growth and composition of the kelp Saccharina latissima. J. Appl. Phycol. 24, 759–776. https://doi.org/10.1007/s10811-011-9695-y.
Burgman, M.A., Gerard, V.A., 1990. A stage-structured, stochastic population model for the giant kelpMacrocystis pyrifera. Mar. Biol. 105, 15–23. https://doi.org/10.1007/BF01344266.
Burrows, M.T., 2012. Influences of wave fetch, tidal flow and ocean colour on subtidal rocky communities. Mar. Ecol. Prog. Ser. 445, 193–207. https://doi.org/10.3354/meps09422.
Burrows, M.T., Fox, C., Moore, P.J., Smale, D.A., Greenhill, L., Martino, S., 2018. Wild seaweed harvesting as a diversification opportunity for fishermen 184.
Burrows, M.T., Harvey, R., Robb, L., 2008. Wave exposure indices from digital coastlines and the prediction of rocky shore community structure. Mar. Ecol. Prog. Ser. 353, 1–12. https://doi.org/10.3354/meps07284.
Capdevila, P., Linares, C., Aspillaga, E., Riera, J.L., Hereu, B., 2018. Effective dispersal and density-dependence in mesophotic macroalgal forests: insights from the Mediterranean species Cystoseira zosteroides. PLoS One 13, e0191346. https://doi.org/10.1371/journal.pone.0191346.
Catherall, unpublished. Unpublished L. hyperborea surveys.
Christie, H., Andersen, G.S., Bekkby, T., Fagerli, C.W., Gitmark, J.K., Gundersen, H., Rinde, E., 2019. Shifts between sugar kelp and turf algae in Norway: regime shifts or fluctuations between different opportunistic seaweed species? Front. Mar. Sci. 6, 72. https://doi.org/10.3389/fmars.2019.00072.
Christie, H., Fredriksen, S., Rinde, E., 1998. Regrowth of kelp and colonization of epiphyte and fauna community after kelp trawling at the coast of Norway. In: Baden, S., Phil, L., Rosenberg, R., Strömberg, J.-O., Svane, I., Tiselius, P. (Eds.), Recruitment, Colonization and Physical-Chemical Forcing in Marine Biological Systems. Springer Netherlands, Dordrecht, pp. 49–58. https://doi.org/10.1007/978-94-017-2864-5_4.
Christie, H., Jørgensen, N.M., Norderhaug, K.M., Waage-Nielsen, E., 2003. Species distribution and habitat exploitation of fauna associated with kelp (Laminaria Hyperborea) along the Norwegian Coast. J. Marine Biol. Assoc. United Kingdom 83, 687–699. https://doi.org/10.1017/S0025315403007653h.
Dayton, P.K., 1985. Ecology of kelp communities. Annu. Rev. Ecol. Syst. 16, 215–245. https://doi.org/10.1146/annurev.es.16.110185.001243.
Denny, M.W., Hunt, L.J.H., Miller, L.P., Harley, C.D.G., 2009. On the prediction of extreme ecological events. Ecol. Monogr. 79, 397–421. https://doi.org/10.1890/08-0579.1.
Desmond, M.J., Pritchard, D.W., Hepburn, C.D., 2017. Light dose versus rate of delivery: implications for macroalgal productivity. Photosynth. Res. 132, 257–264. https://doi.org/10.1007/s11120-017-0381-z.
Duarte, P., Ferreira, J.G., 1997. A model for the simulation of macroalgal population dynamics and productivity. Ecol. Modell. 98, 199–214. https://doi.org/10.1016/S0304-3800(96)01915-1.
Duggins, D., Eckman, J., Siddon, C., Klinger, T., 2003. Population, morphometric and biomechanical studies of three understory kelps along a hydrodynamic gradient. Mar. Ecol. Prog. Ser. 265, 57–76. https://doi.org/10.3354/meps265057.
Elith, J., Leathwick, J.R., Hastie, T., 2008. A working guide to boosted regression trees. J. Anim. Ecol. 77, 802–813. https://doi.org/10.1111/j.1365-2656.2008.01390.x.
Feser, F., Barcikowska, M., Krueger, O., Schenk, F., Weisse, R., Xia, L., 2015. Storminess over the North Atlantic and northwestern Europe—a review. Q.J.R. Meteorol. Soc 141, 350–382. https://doi.org/10.1002/qj.2364.

Feser, F., Krueger, O., Woth, K., van Garderen, L., 2021. North Atlantic winter storm activity in modern reanalyses and pressure-based observations. J. Clim. 34, 2411–2428. https://doi.org/10.1175/JCLI-D-20-0529.1.
Filbee-Dexter, K., Scheibling, R., 2012. Hurricane-mediated defoliation of kelp beds and pulsed delivery of kelp detritus to offshore sedimentary habitats. Mar. Ecol. Prog. Ser. 455, 51–64. https://doi.org/10.3354/meps09667.
Filbee-Dexter, K., Wernberg, T., Grace, S.P., Thormar, J., Fredriksen, S., Narvaez, C.N., Feehan, C.J., Norderhaug, K.M., 2020. Marine heatwaves and the collapse of marginal North Atlantic kelp forests. Sci. Rep. 10, 13388. https://doi.org/10.1038/s41598-020-70273-x.
Fredriksen, S., Sjøtun, K., Lein, T.E., Rueness, J., 1995. Spore dispersal in Laminaria hyperborea (Laminariales, Phaeophyceae). Sarsia 80, 47–53. https://doi.org/10.1080/00364827.1995.10413579.
GEBCO, C.G., 2021. GEBCO 2021 Grid. DOI: 0.5285/c6612cbe-50b3-0cff-e053-6c86abc09f8f.
Gilpin, M.E., Ayala, F.J., 1973. Global models of growth and competition. Proc. Natl. Acad. Sci. USA 70, 3590–3593. https://doi.org/10.1073/pnas.70.12.3590.
Gouraguine, A., Moore, P.J., Burrows, M.T., Velasco, E., Ariz, L., Figueroa-Fábrega, L., Muñoz-Cordovez, R., Fernandez-Cisternas, I., Smale, D.A., Pérez-Matus, A., 2021. The intensity of kelp harvesting shapes the population structure of the foundation species Lessonia trabeculata along the Chilean coastline. Mar. Biol. 168, 66. https://doi.org/10.1007/s00227-021-03870-7.
Harrer, S.L., Reed, D.C., Holbrook, S.J., Miller, R.J., 2013. Patterns and controls of the dynamics of net primary production by understory macroalgal assemblages in giant kelp forests. J. Phycol. 49, 248–257. https://doi.org/10.1111/jpy.12023.
Hereward, H.F.R., King, N.G., Smale, D.A., 2020. Intra-Annual variability in responses of a canopy forming kelp to cumulative low tide heat stress: implications for populations at the trailing range edge. J. Phycol. 56, 146–158. https://doi.org/10.1111/jpy.12927.
Hilde, C.H., Gamelon, M., Sæther, B.E., Gaillard, J.M., Yoccoz, N.G., Pélabon, C., 2020. The demographic buffering hypothesis: evidence and challenges. Trends Ecol. Evol. (Amst.) 35, 523–538. https://doi.org/10.1016/j.tree.2020.02.004.
Kain, J.M., 1979. A view of the genus Laminaria. Oceanogr. Mar. Biol. Ann. Rev. 17, 101–161.
Kain, J.M., 1977. The biology of *Laminaria hyperborea* X. The effect of depth on some populations. J. Mar. Biol. Ass. 57, 587–607. https://doi.org/10.1017/S0025315400025054.
Kain, J.M., 1976a. The biology of Laminaria Hyperborea . VIII. Growth on cleared areas. J. Mar. Biol. Ass. 56, 267–290. https://doi.org/10.1017/S0025315400018907.
Kain, J.M., 1976b. The biology of *Laminaria hyperborea* IX. Growth pattern of fronds. J. Mar. Biol. Ass. 56, 603–628. https://doi.org/10.1017/S0025315400020683.
Kain, J.M., 1975. The biology of *Laminaria hyperborea* VII. Reproduction of the sporophyte. J. Mar. Biol. Ass. 55, 567–582. https://doi.org/10.1017/S0025315400017264.
Kain, J.M., 1969. The Biology of *Laminaria hyperborea* . V. Comparison with early stages of competitors. J. Mar. Biol. Ass. 49, 455–473. https://doi.org/10.1017/S0025315400036031.
Kain, J.M., 1963. Aspects of the biology of *Laminaria Hyperborea : II.* age, weight and length. J. Mar. Biol. Ass. 43, 129–151. https://doi.org/10.1017/S0025315400005312.
Kain, J.M., 1962. Aspects of the biology of *Laminaria hyperborea* I. vertical distribution. J. Mar. Biol. Ass. 42, 377–385. https://doi.org/10.1017/S0025315400001363.
King, N.G., Uribe, R., Moore, P.J., Earp, H.S., Gouraguine, A., Hinostroza, D., Perez-Matus, A., Smith, K., Smale, D.A., 2023. Multiscale spatial variability and stability in the structure and diversity of bacterial communities associated with the Kelp Eisenia cokeri in Peru. Microb. Ecol. https://doi.org/10.1007/s00248-023-02262-2.
Kitching, J.A., 1937. Studies in sublittoral ecology: II. Recolonization at the upper margin of the Sublittoral region; with a note on the denudation of laminaria forest by storms. J. Ecol. 25, 482–495. https://doi.org/10.2307/2256206.
Koehl, M.A.R., Silk, W.K., Liang, H., Mahadevan, L., 2008. How kelp produce blade shapes suited to different flow regimes: a new wrinkle. Integr. Comp. Biol. 48, 834–851. https://doi.org/10.1093/icb/icn069.
Krumhansl, K.A., Lauzon-Guay, J.S., Scheibling, R.E., 2014. Modeling effects of climate change and phase shifts on detrital production of a kelp bed. Ecology 95, 763–774. https://doi.org/10.1890/13-0228.1.
Krumhansl, K.A., Scheibling, R.E., 2012. Production and fate of kelp detritus. Mar. Ecol. Prog. Ser. 467, 281–302. https://doi.org/10.3354/meps09940.
Morris, W.K., Doak, D.F., Sunderland, M.A., 2003. Quantitative Conservation Biology: Theory and Practice of Population Viability Analysis. Sinauer Associates, Inc. Publishers. https://doi.org/10.22621/cfn.v119i2.137.
NASA, 2018. Moderate-resolution imaging spectroradiometer (MODIS) aqua. https://doi.org/10.5067/AQUA/MODIS/L3M.
Nisbet, R.M., Bence, J.R., 1989. Alternative dynamic regimes for canopy-forming kelp: a variant on density-vague population regulation. Am. Nat. 134, 377–408.
Norton, T.A., 1992. Dispersal by macroalgae. British Phycological J. 27, 293–301.
Pedersen, M.F., Filbee-Dexter, K., Frisk, N.L., Sárossy, Z., Wernberg, T., 2021. Carbon sequestration potential increased by incomplete anaerobic decomposition of kelp detritus. Mar. Ecol. Prog. Ser. 660, 53–67. https://doi.org/10.3354/meps13613.
Pedersen, M.F., Nejrup, L.B., Fredriksen, S., Christie, H., Norderhaug, K., 2012. Effects of wave exposure on population structure, demography, biomass and productivity of the kelp Laminaria hyperborea. Mar. Ecol. Prog. Ser. 451, 45–60. https://doi.org/10.3354/meps09594.
Pereira, T.R., Engelen, A.H., Pearson, G.A., Valero, M., Serrão, E.A., 2017. Population dynamics of temperate kelp forests near their low-latitude limit. Aquat. Bot. 139, 8–18. https://doi.org/10.1016/j.aquabot.2017.02.006.
Pessarrodona, A., Foggo, A., Smale, D.A., 2019. Can ecosystem functioning be maintained despite climate-driven shifts in species composition? Insights from novel marine forests. J. Ecol. 107, 91–104. https://doi.org/10.1111/1365-2745.13053.
Pessarrodona, A., Moore, P.J., Sayer, M.D.J., Smale, D.A., 2018. Carbon assimilation and transfer through kelp forests in the NE Atlantic is diminished under a warmer ocean climate. Glob. Change Biol 24, 4386–4398. https://doi.org/10.1111/gcb.14303.
Prowse, T.A.A., Bradshaw, C.J.A., Delean, S., Cassey, P., Lacy, R.C., Wells, K., Aiello-Lammens, M.E., Akçakaya, H.R., Brook, B.W., 2016. An efficient protocol for the global sensitivity analysis of stochastic ecological models. Ecosphere 7, e01238. https://doi.org/10.1002/ecs2.1238.
Reed, D.C., Kinlan, B.P., Raimondi, P.T., Washburn, L., Gaylord, B., Drake, P.T., 2006. A metapopulation perspective on the patch dynamics of giant kelp in southern California, in: marine metapopulations. Elsevier 353–386. https://doi.org/10.1016/B978-012088781-1/50013-3.
Reed, D.C., Laur, D.R., Ebeling, A.W., 1988. Variation in algal dispersal and recruitment: the importance of episodic events. Ecol. Monogr. 58, 321–335. https://doi.org/10.2307/1942543.
Reed, D.C., Schroeter, S.C., Raimondi, P.T., 2004. Spore supply and habitat availability as sources of recruitment limitation in the giant kelp Macrocystis pyrifera (Phaeophyceae). J. Phycol. 40, 275–284. https://doi.org/10.1046/j.1529-8817.2004.03119.x.
Roughgarden, J., Iwasa, Y., Baxter, C., 1985. Demographic theory for an open marine population with space-limited recruitment. Ecology 66, 54–67. https://doi.org/10.2307/1941306.
Shoemaker, L.G., Sullivan, L.L., Donohue, I., Cabral, J.S., Williams, R.J., Mayfield, M.M., Chase, J.M., Chu, C., Harpole, W.S., Huth, A., HilleRisLambers, J., James, A.R.M., Kraft, N.J.B., May, F., Muthukrishnan, R., Satterlee, S., Taubert, F., Wang, X., Wiegand, T., Yang, Q., Abbott, K.C., 2020. Integrating the underlying structure of stochasticity into community ecology. Ecology 101, 1–17. https://doi.org/10.1002/ecy.2922.
Sjøtun, K., Christie, H., Helge Fosså, J., 2006. The combined effect of canopy shading and sea urchin grazing on recruitment in kelp forest (*Laminaria hyperborea*). Mar. Biol. Res. 2, 24–32. https://doi.org/10.1080/17451000500537418.
Sjøtun, K., Fredriksen, S., 1995. Growth allocation in Laminaria hyperborea (Laminariales, Phaeophyceae) in relation to age and wave exposure. Mar. Ecol. Prog. Ser. 126, 213–222. https://doi.org/10.3354/meps126213.
Smale, D.A., 2020. Impacts of ocean warming on kelp forest ecosystems. New Phytol. 225, 1447–1454. https://doi.org/10.1111/nph.16107.
Smale, D.A., Burrows, M.T., Evans, A.J., King, N.G., Sayer, M.D.J., Yunnie, A.L.E., Moore, P.J., 2016. Linking environmental variables with regional- scale variability in ecological structure and standing stock of carbon within UK kelp forests. Mar. Ecol. Prog. Ser. 542, 79–95. https://doi.org/10.3354/meps11544.
Smale, D.A., Pessarrodona, A., King, N., Burrows, M.T., Yunnie, A., Vance, T., Moore, P., 2020. Environmental factors influencing primary productivity of the forest-forming kelp Laminaria hyperborea in the northeast Atlantic. Sci. Rep. 10, 12161. https://doi.org/10.1038/s41598-020-69238-x.
Smale, D.A., Pessarrodona, A., King, N., Moore, P.J., 2021. Examining the production, export, and immediate fate of kelp detritus on open-coast subtidal reefs in the Northeast Atlantic. Limnol. Oceanography lno.11970. https://doi.org/10.1002/lno.11970.
Smale, D.A., Vance, T., 2016. Climate-driven shifts in species' distributions may exacerbate the impacts of storm disturbances on North-east Atlantic kelp forests. Mar. Freshwater Res. 67, 65. https://doi.org/10.1071/MF14155.
Smith, K.E., Moore, P.J., King, N.G., Smale, D.A., 2022. Examining the influence of regional-scale variability in temperature and light availability on the depth distribution of subtidal kelp forests. Limnol. Oceanography 67, 314–328. https://doi.org/10.1002/lno.11994.
Steen, H., Moy, F.E., Bodvin, T., Husa, V., 2016. Regrowth after kelp harvesting in Nord-Trøndelag, Norway. ICES J. Mar. Sci. 73, 2708–2720. https://doi.org/10.1093/icesjms/fsw130.
Steneck, R.S., Graham, M.H., Bourque, B.J., Corbett, D., Erlandson, J.M., Estes, J.A., Tegner, M.J., 2002. Kelp forest ecosystems: biodiversity, stability, resilience and future. Envir. Conserv. 29, 436–459. https://doi.org/10.1017/S0376892902000322.
Szewczyk, T.M., Lee, T., Ducey, M.J., Aiello-Lammens, M.E., Bibaud, H., Allen, J.M., 2019. Local management in a regional context: simulations with process-based species distribution models. Ecol. Modell. 413, 108827 https://doi.org/10.1016/j.ecolmodel.2019.108827.
Teagle, H., Moore, P.J., Jenkins, H., Smale, D.A., 2018. Spatial variability in the diversity and structure of faunal assemblages associated with kelp holdfasts (Laminaria hyperborea) in the northeast Atlantic. PLoS One 13, e0200411. https://doi.org/10.1371/journal.pone.0200411.
Terry, J.C.D., O'Sullivan, J.D., Rossberg, A.G., 2022. Synthesising the multiple impacts of climatic variability on community responses to climate change. Ecography e06123. https://doi.org/10.1111/ecog.06123, 2022.
van Sebille, E., Griffies, S.M., Abernathey, R., Adams, T.P., Berloff, P., Biastoch, A., Blanke, B., Chassignet, E.P., Cheng, Y., Cotter, C.J., Deleersnijder, E., Döös, K., Drake, H.F., Drijfhout, S., Gary, S.F., Heemink, A.W., Kjellsson, J., Koszalka, I.M., Lange, M., Lique, C., MacGilchrist, G.A., Marsh, R., Mayorga Adame, C.G., McAdam, R., Nencioli, F., Paris, C.B., Piggott, M.D., Polton, J.A., Rühs, S., Shah, S.H.A.M., Thomas, M.D., Wang, J., Wolfram, P.J., Zanna, L., Zika, J.D., 2018. Lagrangian ocean analysis: fundamentals and practices. Ocean Modell. 121, 49–75. https://doi.org/10.1016/j.ocemod.2017.11.008.
Venolia, C.T., Lavaud, R., Green-Gavrielidis, L.A., Thornber, C., Humphries, A.T., 2020. Modeling the growth of sugar kelp (Saccharina latissima) in aquaculture systems

using dynamic energy budget theory. Ecol. Modell. 430, 109151 https://doi.org/10.1016/j.ecolmodel.2020.109151.
Walker, F.T., 1954. The Laminariaceae off North Shapinsay: changes from 1947 to 1953. Ann. Bot. 18, 483–494. https://doi.org/10.1093/oxfordjournals.aob.a083411.
Wernberg, T., Vanderklift, M.A., 2010. Contribution of temporal and spatial components to morphological variation in the kelp Ecklonia (Laminariales). J. Phycol. 46, 153–161. https://doi.org/10.1111/j.1529-8817.2009.00772.x.
Westermeier, R., Murúa, P., Patiño, D.J., Manoli, G., Müller, D.G., 2019. Evaluation of kelp harvest strategies: recovery of Lessonia berteroana (Phaeophyceae, Laminariales) in Pan de Azucar, Atacama, Chile. J. Appl. Phycol. 31, 575–585. https://doi.org/10.1007/s10811-018-1500-8.
Wing, S.R., Leichter, J.J., Denny, M.W., 1993. A dynamic model for wave-induced light fluctuations in a kelp forest. Limnol. Oceanogr. 38, 396–407. https://doi.org/10.4319/lo.1993.38.2.0396.